scientific reports

Check for updates

OPEN

Glutaminase inhibitor CB-839 causes metabolic adjustments in colorectal cancer cells

Martina Spada[1], Cristina Piras[1]✉, Vera Piera Leoni[1], Mattia Casula[2], Gabriella Simbula[1], Antonio Noto[1], Katia Lilliu[1], Karolina Krystyna Kopeć[3], Gabriele Serreli[1], Federica Murgia[4], Federica Etzi[1], Tinuccia Dettori[1], Luigi Atzori[1,5] & Paola Caria[1,5]

Colorectal cancer (CRC) cells are 'addicted' to glutamine to satisfy energy and biosynthetic needs. Inhibiting glutamine metabolism enzymes, like glutaminase, is a potential cancer therapy strategy. Although the GLS inhibitor CB-839 is being evaluated in clinical trials, a comprehensive assessment of its antitumor activity in CRC cells is crucial. The present study aimed to evaluate the impact of CB-839 treatment on different CRC cell lines in terms of survival and proliferation. Furthermore, metabolic adaptations resulting from CB-839 treatment, particularly in energetic pathways, were investigated. Three CRC cell lines (HCT116, HT29, and SW480) were treated with different CB-839 concentrations. Cytotoxicity was assessed via MTT assay, proliferation capacity by flow cytometry, and ATP production rates by Seahorse XF analysis. Moreover, metabolomic profile was explored with untargeted GC-MS and ^{1}H-NMR, and targeted analysis of the Krebs cycle was conducted using GC-MS/MS. HT29 cells exhibited the highest sensitivity to CB-839. Subsequent experiments focused on HT29 and SW480 cells. CB-839 treatment altered cell cycle progression and increased glycolytic ATP production in HT29 cells. Metabolomic analysis revealed changes in Krebs cycle and glutaminolysis in both cell lines, along with alterations in amino acids, sugars, antioxidants, and organic acid levels. This study highlighted glutamine's key role in CRC cells and provided a foundation for elucidating the mechanisms of response and resistance to CB-839.

Keywords Colorectal cancer, Glutamine metabolism, CB-839, Glutaminolysis, Glutaminase-1 inhibition, Energetic metabolism

Colorectal cancer (CRC) is the second deadliest cancer and the third most diagnosed malignancy worldwide[1]. Thanks to screening programs and early diagnosis, mortality rates have decreased overall. Unfortunately, the incidence rate in young patients (under 50 years old) has increased[2,3]. It is currently known that cancer cells rewire their metabolism to cope with rapid growth and proliferation[4]. Tumour cells prioritize different energy sources than normal cells to meet the high energetic and biosynthetic demand[5]. Indeed, it has been found that among these alternative sources, glutamine plays a pivotal role in supporting cancer growth and proliferation[6]. Several tumor types become addicted to this amino acid[7], including CRC cells[8]. Particularly, glutamine represents a carbon and nitrogen source necessary for amino acid, nucleotide and lipid biosynthesis. In addition, glutamate produced by glutamine deamination can be converted into α-ketoglutarate, supporting energy production by fueling the Krebs cycle. Furthermore, the glutamine-derived glutamate can be used as a glutathione constituent, thus participating in redox homeostasis[7]. The mitochondrial enzyme glutaminase (GLS) is responsible for converting glutamine into glutamate, thus performing the first and rate-limiting step of glutamine metabolism. Two main isoforms of glutaminase have been described in mammals: GLS-1(kidney-type) and GLS-2 (liver-type), which differ in kinetic properties, protein structures, and tissue distribution[9,10]. Over-expression of the GLS-1 enzyme correlates with poor prognosis and overall low survival in different types of cancer, including breast, ovarian, and CRC[11,12]. The metabolic vulnerabilities of cancer raised interest in the development of metabolism-targeted therapies. Targeting glutamine metabolism represents an attractive and promising strategy in cancer therapy due to the central role played by this amino acid. To date, several drugs impairing glutamine metabolism have been introduced in clinical trials for various tumor types, including CRC[13]. Among these

[1]Department of Biomedical Sciences, University of Cagliari, Cagliari, Italy. [2]Department of Life and Environmental Sciences, University of Cagliari, Cagliari, Italy. [3]Department of Mechanical, Chemical and Materials Engineering, University of Cagliari, Cagliari, Italy. [4]Laboratory Medicine, Santissima Trinità Hospital, Cagliari, Italy. [5]Luigi Atzori and Paola Caria contributed equally to this work. ✉email: cristina.piras@unica.it

drugs, Telaglenastat (CB-839) has emerged as one of the most promising drugs and represents a potent, selective, reversible, and orally bioavailable inhibitor of GLS-1[14]. Currently, CB-839 is reporting promising results in various types of solid tumors (triple-negative breast cancer, ovarian cancer, non-small cell lung cancer) and hematological malignancies. In particular, its combinatorial efficacy with chemotherapies and other molecularly targeted agents is being tested in late-stage clinical trials[15–18]. Despite its efficacy in various neoplasms, the antitumoral effect of CB-839 in CRC cells has been poorly evaluated in CRC cells, and few studies on this type of tumor are present in the scientific literature[19,20]. New findings could therefore help to improve targeted therapy in CRC patients and contribute to the development of innovative combination therapies. In the present study, we evaluated the effect of CB-839 on proliferation and the metabolic effects of inhibiting GLS-1 activity on various CRC cells.

Results

CB-839 exerted cytotoxic effects on CRC cells

To investigate whether CB-839 exerted cytotoxic effects on CRC cells, cell viability was assessed on CRC cell lines using the MTT assay. The results showed that CB-839 treatment decreased the viability in the HT29 cell line in a dose-dependent manner (Fig. 1). Moreover, the cytotoxic effect of CB-839 on HT29 cells was stronger after 96 h of treatment (CC_{50} = 8.75 µM) than after 48 h (CC_{50} = 19.10 µM). SW480 cells were the least sensitive and required a higher drug concentration to achieve a 50% viability reduction. Surprisingly, the CC_{50} was higher after 96 h (CC_{50} = 51.41 µM) than after 48 h of treatment (CC50 = 37.48 µM). Lastly, HCT116 cells were modestly sensitive to the drug (CC_{50} = 43.26 µM at 48 h and CC_{50} = 26.31 µM at 96 h). These results prompted us to select HT29 and SW480 cells, the most and the least sensitive cell lines, to further investigate CB-839 effects. All following experiments were performed exposing HT29 and SW480 at different CB-839 concentrations to investigate changes occurring after a cytotoxic or an adaptive response.

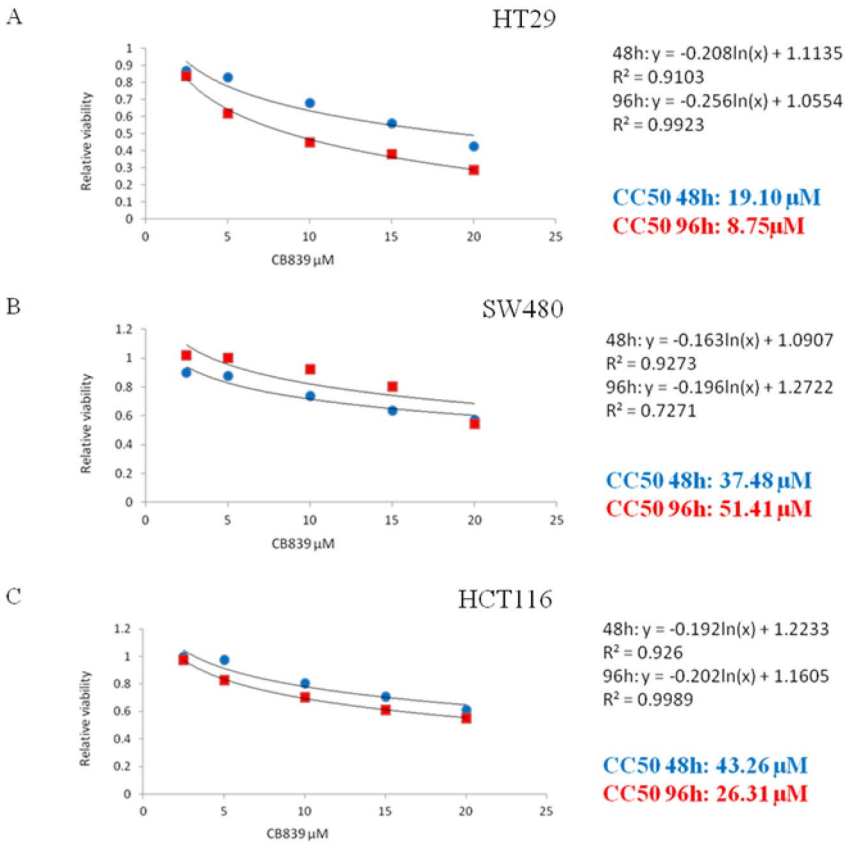

Fig. 1. Cell viability curves of colorectal cancer cell lines: (**A**) HT29; (**B**) SW480; (**C**) HCT116 after CB-839 treatment. Cell viability was assessed by MTT assay at 48 h in blue and 96 h in red at different CB-938 concentrations, reported in the x-axis. Representative growth curves of three independent experiments are shown. Data are presented as means of at least 4 replicates. On the right, the equation of the curve and the corresponding correlation coefficient for 48 h and 96 h were reported for each cell line.

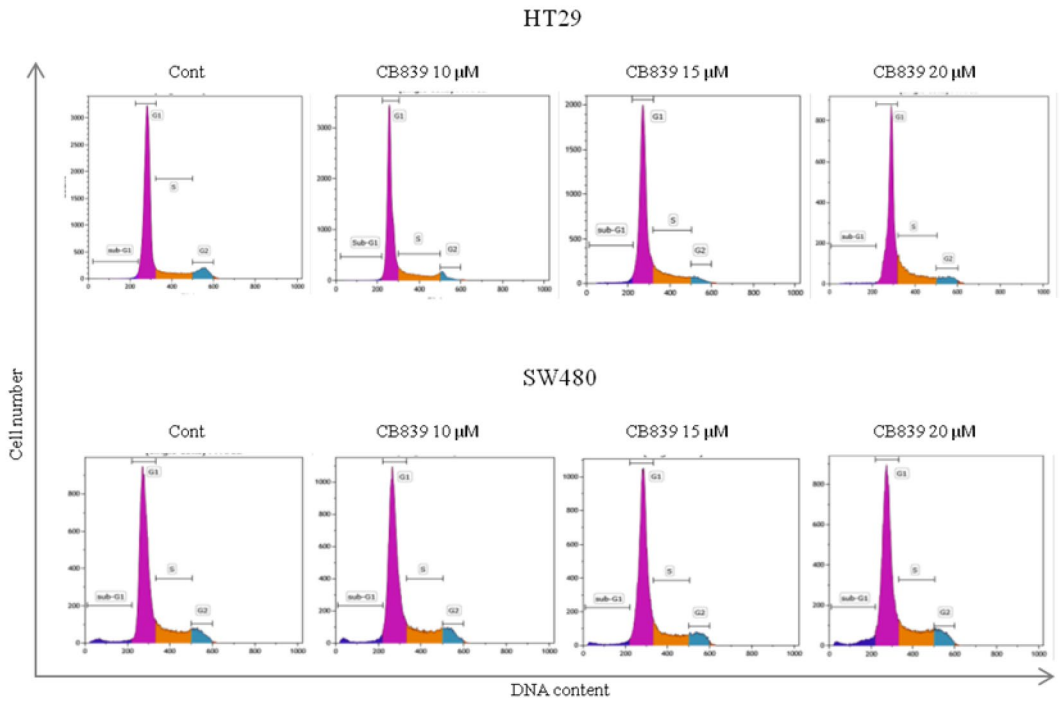

Fig. 2. Flow cytometry analysis of cell cycle distribution in HT29 and SW480 cells exposed for 48 h to different CB-839 concentrations (10-15-20 μM). The result of one representative assay from three similar independent experiments is shown. *x*- and *y*-axes indicate cell number and DNA content, respectively.

Cell line		Sub-G0 Phase		G0/G1 Phase		S Phase		G2/M Phase	
		% of cells ± SD	p-value (vs. Cont)	% of cells ± SD	p-value (vs. Cont)	% of cells ± SD	p-value (vs. Cont)	% of cells ± SD	p-value (vs. Cont)
HT29	Cont	0.73 ± 0.18		74.41 ± 0.36		14.4 0 ± 0.22		9.92 ± 0.51	
	CB-839 10 μM	1.28 ± 0.17	*ns*	76.74 ± 0.19	*ns*	16.31 ± 0.22	*ns*	5.45 ± 0.32	0.0002
	CB-839 15 μM	2.91 ± 0.72	0.0006	73.99 ± 2.82	*ns*	18.20 ± 1.30	0.0014	4.62 ± 1.02	0.0001
	CB-839 20 μM	2.14 ± 0.37	0.0091	67.41 ± 1.35	*ns*	24.78 ± 1.00	0.0001	6.58 ± 1.00	0.0020
SW480	Cont	3.69 ± 0.45		65.41 ± 1.22		21.96 ± 0.64		8.71 ± 1.10	
	CB-839 10 μM	4.18 ± 0.52	*ns*	67.34 ± 1.13	*ns*	20.12 ± 1.54	*ns*	9.35 ± 0.66	*ns*
	CB-839 15 μM	3.38 ± 0.66	*ns*	65.08 ± 0.62	*ns*	21.55 ± 0.28	*ns*	9.31 ± 0.90	*ns*
	CB-839 20 μM	5.02 ± 1.14	*ns*	62.57 ± 2.03	*ns*	22.92 ± 1.32	*ns*	8.76 ± 0.13	*ns*

Table 1. Effects of CB-839 on the cell cycle distribution of CRC cell lines. CRC cells were treated with different concentrations of CB-839 for 48 h, stained with propidium iodide, and subjected to flow cytometric analysis. Experiments were performed in triplicate and data were expressed as cell percentages and represent mean ± SD; ns: not significant.

CB-839 altered cell cycle progression in HT29 cells

Based on the results of cell viability, a reduction in proliferation capacity due to CB-839 was assumed. After 48 h of treatment, the distribution of HT29 and SW480 cell lines in the different phases of the cell cycle was explored by FACS analysis. The HT29 cells accumulated in the S phase in a dose-dependent way after the treatment, and at the same time, a reduction of the cell percentage in the mitotic phase (G2/M) was observed (Fig. 2). Moreover, an increase in the sub-G0 phase was observed in HT29 cells. No significant alterations in cell cycle progression were noticed in SW480 cells after the treatment. Detailed information on the cell percentage distribution and the relative statistical significance is reported in Table 1.

CB-839 treatment led to metabolic rewiring in CRC cells

Considering the key role of glutamine in energetic and biosynthetic processes, the metabolomic profile was explored through an untargeted GC-MS and ^{1}H-NMR analysis. All identified metabolites and their relative

concentrations were merged and scaled into a single matrix, before being subjected to statistical analysis. The unsupervised PCA was performed and as shown in Fig. 3, a good separation between control and treated groups was observed in both HT29 (Fig. 3A) and SW480 (Fig. 3B) cell lines. This observed distribution suggested that GLS-1 inhibition exerted a strong influence on CRC cell metabolism. Moreover, the spatial disposition of the different groups of cells in the score plot reflected the rising drug concentrations, suggesting a dose-dependent metabolic response.

Subsequently, univariate statistical analysis was performed to identify which metabolites were mostly affected by the treatment and, thus, responsible for the separation. Specifically, the ANOVA test was performed for each metabolite, and the treated groups were compared to the respective control. The analysis showed extensive metabolic rewiring in both CRC cells after CB-839 treatment. A schematic representation of the main metabolic alterations observed in the two cell lines after CB-839 treatment is reported in Fig. 4. A detailed list of identified metabolites, trend of alterations, and statistical parameters is stated in Table 1S. As expected,

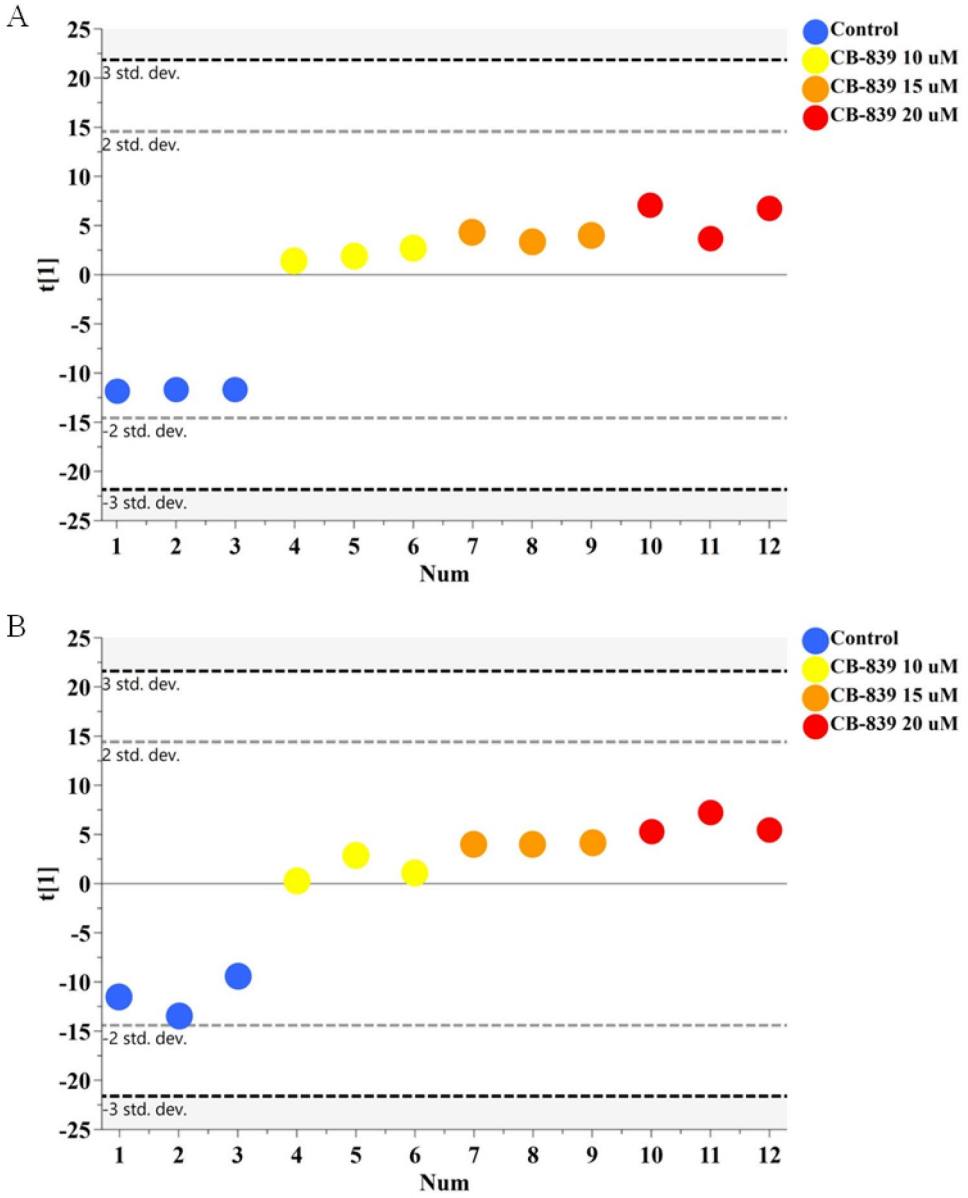

Fig. 3. PCA scores plot based on metabolite concentrations measured by GC-MS and ^{1}H-NMR analysis. The metabolic profile of HT29 (3 A) and SW480 (3B) cells treated with different concentrations of CB-839 (10-15-20 μM) and in control conditions was. The unsupervised analysis showed a good separation among groups and a trend according to the drug concentration. PCA scores plot: 62.4% of total variance explained for HT29 and 60.3% for SW480.

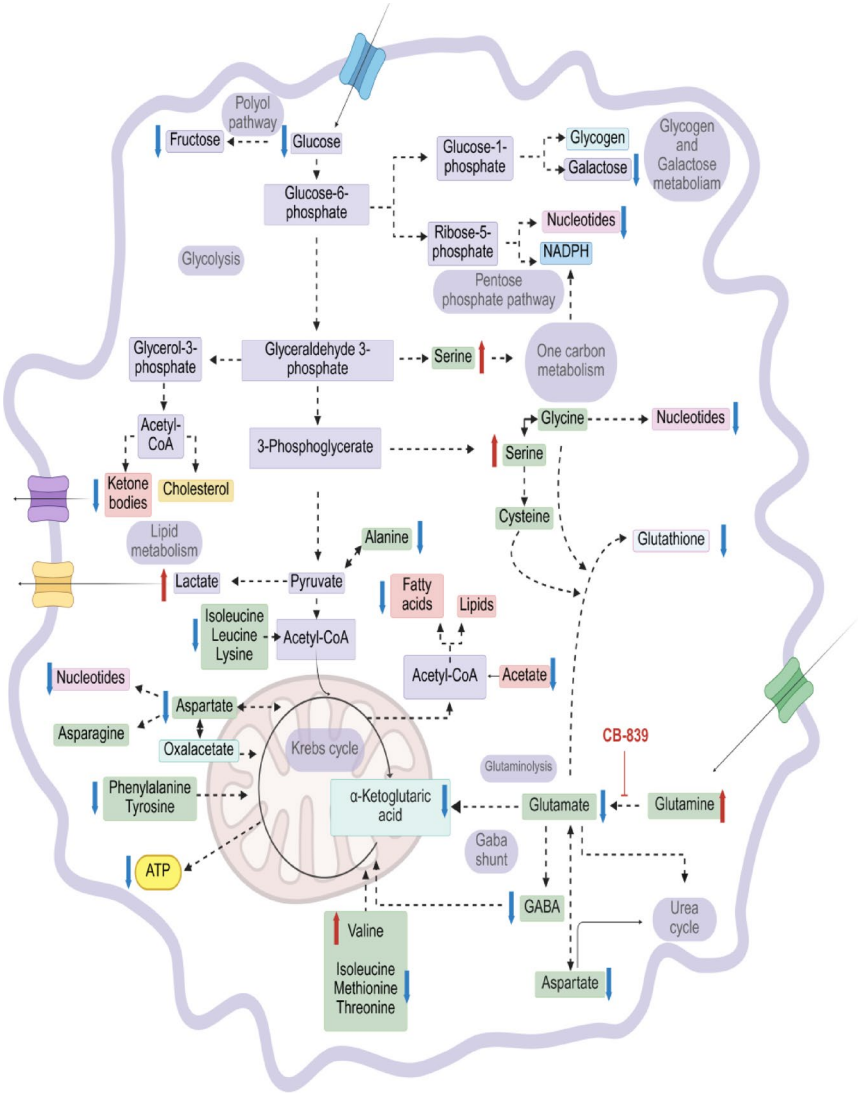

Fig. 4. The figure shows the metabolic pathways mainly involved in the treatment of CRC cells with CB-839. The figure summarizes the alterations presented by both cell lines treated with CB-839 at a concentration of 20 μM. The metabolites found to be significantly modified show an arrow indicating the trend of the alteration, red if the treatment induced an increase in the levels of the metabolite, and blue if there is a reduction in its concentration compared to the control. The complete list of metabolites identified by metabolomic analysis, the relative concentrations for each dose of CB-839 tested, and the statistical parameters for each of the two studied CRC cells are reported in Table 2 S. This image has been created with BioRender.

glutamine concentration increased in treated cells, while glutamate abundance decreased after GLS-1 inhibition. In HT29 cells a reduction of sugar content was observed in treated cells (glucose, fructose, galactose), while in SW480 cells only the glucose amount was decreased. Furthermore, lactic acid intracellular levels increased with treatment. The results of the metabolic analysis suggest a decrease in energy substrate content in the form of ATP due to CB-839. Moreover, the aminoacidic pool was deeply altered after GLS-1 inhibition, in particular, alanine, aspartate, isoleucine, methionine, and tyrosine showed a strong reduction in both cell lines. Other amino acids displaying a severe decrease after treatment were glycine, ornithine, and phenylalanine. Leucine, lysine, and threonine were only found strongly reduced in HT29 cells, while proline decreased mainly in SW480 cells. Serine and valine were the only two amino acids significantly increased, but only in HT29 cells and after the treatment with the highest concentration of the drug. The monophosphate nucleotides, inosine, and uridine monophosphate (IMP and UMP, respectively) were significantly decreased after the treatment. Concerning fatty acid metabolism, a significant decrease in carnitine and several short-chain fatty acids (2-hydroxybutirate, 3-hydroxybutyrate, 3-methyl-2-oxovalerate) was found in both treated cell lines. Drug treatment caused the alteration of species involved in redox homeostasis, in particular, glutathione content was affected in both cell lines, while NAD^+ and $NADP^+$ were decreased especially in HT29 cells.

CB-839 induced a shift in ATP production from mitochondrial respiration to Glycolysis in HT29 cells

Analysis of the metabolomic profile of CRC cell lines suggested impaired energy production pathways after CB-839 administration. Therefore, the energetic phenotype and its changes in HT29 and SW480 cells after the treatment with 15 μM of CB-839 was evaluated, through the XF Real-Time ATP Rate Assay using the Seahorse Analyzer. Figure 5 shows the extracellular acidification rate and intracellular ATP levels measured after 48 h of treatment with 15 μM CB-839 in HT29 and SW480 cells. A significant decrease in mitochondrial ATP production rates and an increase in glycolytic ATP rates were observed in HT29 cells, after CB-839 treatment. The increase in glycolytic activity of HT29 cells was also confirmed by the significant increase in the extracellular acidification rate, due to the raised release of lactic acid by the cells. In contrast, no significant changes were observed in SW480 cells, and total ATP production rates and the release of lactic acid remained almost constant.

CB-839 impaired Krebs cycle in HT29 and SW480 cells

Considering the metabolic rewiring towards the glycolytic pathway after CB-839 treatment, and the role of glutamine as anaplerotic substrate of tricarboxylic acid (TCA) cycle, the Kreb's cycle intermediates were analyzed through a targeted approach. HT29 and SW480 cells were investigated at three different concentrations of CB-839 (10, 15, and 20 μM) after 48 h of treatment. The targeted analysis showed significant alterations in both tested cell lines, despite the resistance of SW480 cells to CB-839 proliferative inhibitory activity. Specifically, a significant decrease in the levels of TCA intermediates, especially downstream of glutaminolysis in HT29 cells (α-ketoglutaric acid, succinic acid and fumaric acid) was observed. Lower levels of oxaloacetic acid and malic acid were observed at the highest doses of CB-839, while no changes were found in citric acid abundance at different drug concentrations. On the other hand, an alteration in the content of all Krebs cycle intermediates was observed in SW480 cells, as well as citric acid, in contrast to HT29 cells. An overview of Krebs cycle intermediates identified using a targeted approach, and the main anaplerotic pathways, glutaminolysis and GABA shunt, detected with an untargeted approach, in HT29 and SW480 cells were shown in Fig. 6A and B, respectively.

Discussion

In recent years, glutamine metabolism has become an intriguing target in CRC therapy in light of its central role in cell growth and survival[21–24]. Consequently, various molecules impairing glutamine metabolism have been introduced in clinical trials for several tumors, including CRC[13]. Among these drugs, the compound CB-839 has been widely tested alone or in combination with classical antineoplastic agents[15] however, its efficacy

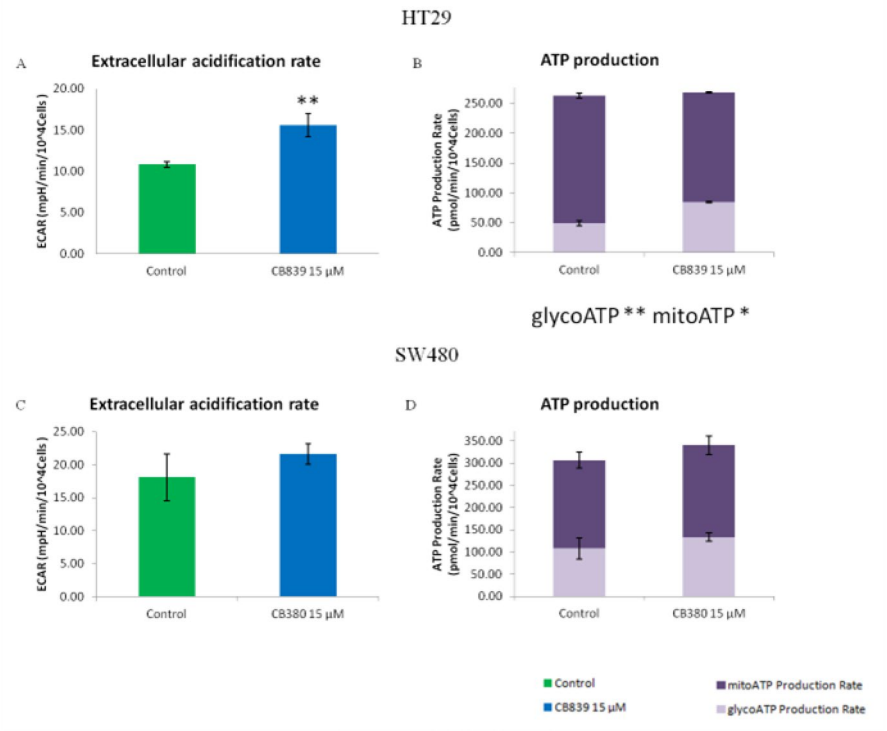

Fig. 5. Quantification of ATP production by Seahorse XF real-time ATP rate assay following 15 μM of CB-839 treatment at 48 h in HT29 and SW480 cells. In (**A**) and (**B**) the extracellular acidification rate and ATP production from mitochondrial and glycolytic pathways, respectively, of HT29 cells are reported. In (C) and (D) the same parameters are reported for SW480 cells. Data are presented as the mean of 3 replicates ± standard deviation. * $p < 0.05$, ** $p < 0.005$.

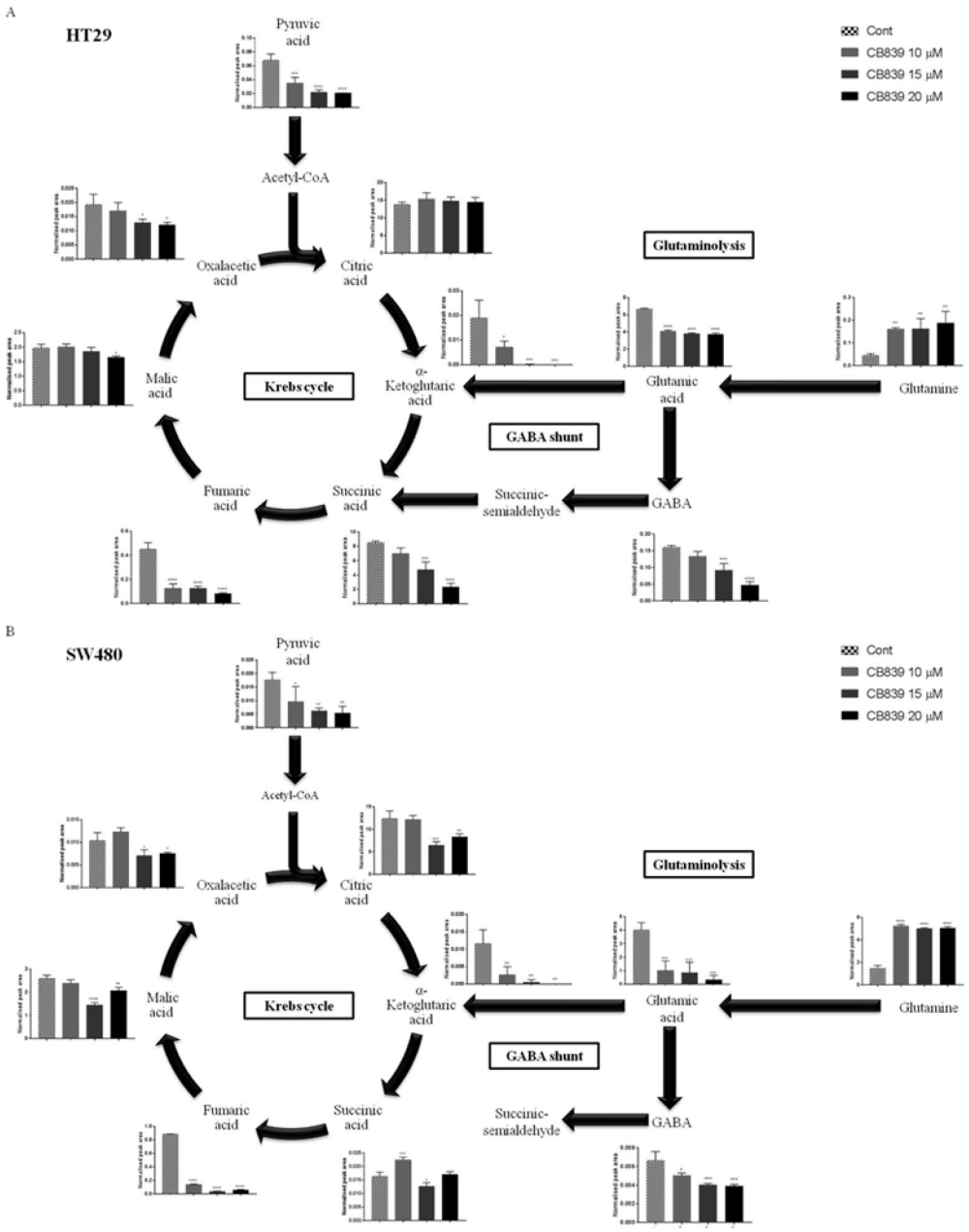

Fig. 6. Targeted metabolomics of Krebs cycle intermediates and untargeted determination of anaplerotic pathways, glutaminolysis, and GABA shunt, in HT29 (**A**) and SW480 (**B**) cells. Histograms represent relative concentrations of intermediate metabolites after 48 h of treatment with CB-839 10, 15, and 20 μM compared to control. Data are presented as the meaning of 3 replicates ± standard deviation. * $p < 0.05$, ** $p < 0.005$, *** $p < 0.0005$, **** $p < 0.0001$).

has been poorly evaluated in CRC. Therefore, the present study aimed to test the efficacy of CB-839 on cell viability, proliferation, and energy metabolism in CRC cell lines. Although all tested cell lines were sensitive to glutamine deprivation[8], HT29 cells were the most sensitive to CB-839 treatment, whereas HCT116 and SW480 cells required higher drug concentrations to achieve 50% inhibition of viability, suggesting that CRC cell lines may rely on different mechanisms to overcome the impairment of glutamine metabolism. Cell cycle progression analysis showed a decrease in proliferative capacity in HT29 cells, with an increase in the S-phase cell percentage and the simultaneous reduction of cells in the G2/M phase, suggesting that HT29 cells entered the S-phase but were not able to complete the replication. During S-phase, cells duplicate their genetic material, and, when DNA breakage occurs, the synthesis is interrupted to allow DNA repair, and consequently S phase is prolonged[25], thus it can be hypothesized that DNA damage occurs after the treatment in HT29 cells. Consistent with our hypothesis, Shen and colleagues[26] demonstrated an increased expression of replication stress response markers (pRPA, γH2AX, and pAT) in ovarian cancer cells after CB-839 treatment. In SW480 cells no significant alterations were

observed in the cell cycle after the treatment, confirming the resistance of SW480 cells to the drug. Moreover, numerous works attribute the arrest of proliferation to the lack of nucleotides, of which glutamine represents the precursor[27–30]. Indeed, metabolomic analysis showed decreased levels of nucleotide precursors, such as inosine and uridine monophosphate. Furthermore, in HT29 cells a significant increase in cell percentage in the sub-G0 phase was observed, especially at high concentrations of the drug. A slight rise, but not statistically significant, was noticed also in SW480 cells. As demonstrated in previous studies[31–33], glutamine plays a critical role in the regulation of apoptosis. The apoptotic programme can be triggered by the increase in ROS species due to the decrease in GSH content[33,34] Accordingly, the decrease of GSH observed in CRC-derived cells emphasises the alteration of the redox balance after treatment with CB-839 and thus its possible involvement in the induction of programmed death mechanisms.

Nowadays, also thanks to the support of artificial intelligence[35], metabolomics can describe the pathological profile[36–38], the response to therapy[39,40] or the physio-pathological mechanisms[41] underlying several morbid conditions. The metabolomic analysis conducted in the present study, which included both untargeted and targeted approaches, revealed numerous and significant changes after CB-839 treatment. The metabolome is extensive and intricated, making it challenging to examine in its entirety. Furthermore, glutamine plays a multifaceted role in cellular and tumor metabolism, contributing to various biosynthetic and energetic processes[7]. Consequently, despite a fair number of metabolites were identified and one of the main pathways of glutamine metabolism, namely glutaminolysis, was investigated, it is possible that the pharmacological inhibition of GLS-1 could impact other metabolites. These alterations may emerge from further studies, Metabolomics was used to understand which mechanisms might underlie the response or resistance to CB-839 treatment in colorectal cancer cells. Metabolic profiling analysis highlighted differences between controls and treated cells, indicating a dose-dependent phenotypic change in CRC cells. As expected, metabolomics investigation showed the accumulation of the substrate (glutamine) and the decrease of the product (glutamate) after GLS-1 inhibition with CB-839. Moreover, several metabolite levels, such as alpha-ketoglutarate and aspartate, linked to glutamate, dropped due to GLS-1 inhibition. Furthermore, the reduction of aspartate concentration was reported, indeed its amino group is transferred by an aminotransferase to alpha-ketoglutarate to produce glutamate[42]. Probably, CRC cells improve aspartate catabolism to counteract glutamate deficit due to CB-839 treatment. Metabolomics analysis highlighted the alteration of the aminoacidic pool. Most of the amino acid levels, such as alanine, glycine, isoleucine, phenylalanine, and tyrosine, were decreased after the treatment. Glutamine-derived glutamate represents the precursor of non-essential amino acids[43], so the lack of this substrate could induce the decrease of the aminoacidic pool in CRC cells. Moreover, it is well known that glutamine deprivation alters amino acid transport[44], thus modifying intracellular amino acid contents. Interestingly, in HT29 cells, serine and valine levels were significantly upregulated while leucine and lysine intracellular content was remarkably diminished. The altered intake and consumption of certain amino acids in the susceptible HT29 cells could be due to stress caused by glutamine metabolism impairment. It can be supposed that HT29 cells enhance leucine catabolism to compensate for the lack of glutamate due to CB-839 treatment, since the leucine amino group is transferred to alpha-ketoglutarate, leading to the production of α-ketoisocapropic acid and glutamate[45]. Polet et al. reported the upregulation of the serine pathway during glutamine withdrawal in leukemia cells to counteract oxidative stress. This raised metabolic activity could justify the increased levels of serine at a high CB-839 doses[46]. The same trend was observed in glioma cells, where serine uptake was upregulated to provide biosynthetic precursors and carbon to fuel one-carbon metabolism[47].

The treatment with CB-839 affects sugars metabolism: HT29 cells showed decrease in glucose, fructose, and galactose levels, while in SW480 only glucose content was reduced. This suggests a raised consumption of carbohydrates to provide carbon for biosynthetic purposes particularly in HT29 cells. Moreover, the increased glucose consumption could be addressed by the raised glycolytic rate, which consumes glucose at a higher rate in comparison to oxidative phosphorylation[48]. The high glycolytic rate in HT29 cells has been confirmed by XF Real-Time ATP Rate Assay analysis, which showed a significant increase in glycolytic activity to produce energy, in the form of ATP. The boosted glycolytic rate after GLS-1 inhibition is confirmed by the increased lactic acid release in the extracellular environment, observed with Seahorse analysis, and by the significant increase of intracellular lactic acid, detected with metabolomic experiments. Mitochondrial ATP production was significantly decreased after CB-839 treatment in HT29 cells indicating the reduction in Krebs' cycle activity. CB-839-induced deregulation of TCA cycle has been previously observed in different cell lines[49,50]. This data was supported by targeted analysis of TCA cycle intermediates, which showed a significant drop in metabolite levels downstream of glutaminolysis. Although Seahorse analysis only displayed a slight alteration of ATP production via oxidative pathway in SW480 cells, surprisingly, targeted analysis showed alterations of Krebs' cycle with reduction of all TCA cycle intermediates after treatment. Interestingly, in SW480 cells, citric acid levels were lower after the treatment, probably due to its anaplerotic role under nutrient-limited conditions. Indeed, it has been shown that exogenous citrate supplementation helps cell growth during stress conditions, fuelling fatty acid synthesis[51]. It can be hypothesized that citrate is redirected to lipid synthesis, and this would represent a mechanism implemented by SW480 cells to counteract glutamine metabolism impairment. Furthermore, after CB-839 treatment a significant decrease of gamma-aminobutyric acid (GABA), a storage molecule for succinate[52], was observed. Cells exploit the pathway called GABA shunt to supply the Krebs cycle and overcome metabolic stress[53,54]. This observation suggests a possible and potential combination of the compound CB-839 with drugs targeting GABA biosynthetic enzymes, providing an important starting point for future studies.

Moreover, HT29 cells showed a significant decrease in NAD^+ and $NADP^+$ content, representing an intriguing difference in the response to CB-839 between HT29 and SW480 cells. NAD^+ was discovered as an electron transporter in redox reactions[55]. Nowadays, it is known that the maintenance of high NAD^+ and $NADP^+$ production is required for numerous cellular processes involved in cancer cell growth and proliferation, such as pentose phosphate pathways, serine biosynthesis and fatty acid synthesis[56,57]. The deficiency of these important

cofactors could be due to their use as electron carriers to compensate for the redox imbalance due to CB-839 treatment. Consequently, the failure of NAD^+ and $NADP^+$ could determine impairment of the pathways that use these cofactors and that contribute to the growth and proliferation of tumor cells. The difference in terms of NAD^+ and $NADP^+$ concentrations between HT29 and SW480 could therefore be responsible for the different responses of the two cell lines and deserves further investigation.

Conclusion

In the present study, the effects of the GLS-1 inhibitor, CB-839 and, therefore, the effects of the impairment of glutamine metabolism in CRC cells were investigated. Specifically, two glutamine-dependent cell lines were compared. Despite the dependence on glutamine, the CRC cells showed different responses to CB-839 treatment. In particular, glutamine metabolism impairment mainly affected proliferation capacity, energy metabolism and ATP production pathways, aminoacidic profile, and redox balance. Although SW480 cells were less sensitive to the drug, they showed profound alterations at the metabolic level similar to HT29 cells. These alterations probably represent an attempt by the cells to adapt and respond to the drug CB-839. On the other hand, the decrease of citrate levels observed in SW480 cells could represent an intriguing mechanism that counteract pharmacological inhibition of GLS-1 and explain at least in part the lower sensitivity to the drug. Moreover, this study revealed an important difference in the response to the drug between the two cell lines, indeed a decrease in NAD^+ and $NADP^+$ was found only in HT29 cells. Considering the fundamental role of these two cofactors in tumour growth and proliferation, it can be assumed that they are involved in the different outcomes of treatment with CB-839. This study serves as a starting point to investigate the efficacy of CB-839 in colorectal cancer and the possible resistance mechanisms of CRC cells. The experiment conducted revealed a reduction of viability and proliferation capacity in HT29 cells and metabolic alterations, both in respondent and resistant cells, following the treatment. However, additional research is required to fully elucidate the underlying mechanisms responsible for these changes and if these alterations are responsible for the different response of studied CRC cells to the drug. Despite these limitations, the study suggests valuable insights for understanding the biochemical characteristics and mechanisms predisposing to drug sensitivity or resistance and offers a strong rationale for promising combined therapy.

Materials and methods

Cell culture and chemicals

HCT116 cells were kindly gifted by Dr. Giuseppina Sanna (University of Cagliari, Italy). HT29 cells were purchased from Elabscience®, Houston, TX, USA. SW480 cells were obtained from the cell bank ICLC (San Martino Polyclinic Hospital, Genova, Italy). The cell lines were maintained and assayed in Dulbecco's Modified Eagle's Medium (DMEM) with high glucose, supplemented with 10% heat-inactivated bovine serum (FBS, Life Technologies, Milan, Italy), 100 U/mL penicillin, 100 mg/mL streptomycin (Sigma-Aldrich, Milan, Italy), L-glutamine 2 mM (Euroclone, Milan, Italy) and sodium pyruvate 1 mM (Euroclone, Milan, Italy), at 37 °C and 5% CO_2. The drug CB-839 was purchased from Sigma-Aldrich, Milan, Italy.

All experiments described in this work were evaluated at 48 h, except for viability assay, which was also assessed at 96 h, as reported in the literature[58–60].

Cell viability assay

For viability assays, HCT116, HT29, and SW480 cells were seeded in 96-well plates (1×10^5 cells/mL; 100 µL/well). The following day cells were treated with different concentrations of CB-839 (2.5, 5, 10, 15, 20 µM) for 48 and 96 h. The cell viability was assessed with MTT (3-[4,5-dimethylthiazol-2-yl]−2,5 diphenyl tetrazolium bromide) assay[61]. Data were expressed as absorbance at 570 nm ± standard deviation. A viability curve was built for each cell line. The CC_{50} (cytotoxicity concentration 50%, i.e. the concentration able to achieve a viability reduction of 50%) was extrapolated from the curve. All experiments were carried out in at least quadruplicate and repeated 3 times.

Fluorescence-Activated cell sorting (FACS) analysis

Cell cycle progression was explored by flow cytometry, using the FxCycle™ PI/RNase Staining Solution kit, as previously described by Dettori and colleagues[62]. Additional information is provided in the supplementary materials.

Metabolomics analysis through GC-MS, ^{1}H-NMR, and GC-MS/MS techniques

The samples were processed for Gas Chromatography-Mass Spectrometry (GC-MS) and ^{1}H-NMR analysis, as described in our previous work[63]. Hydrophilic intracellular metabolites were extracted following the method described by Tronci and colleagues[64]. Untargeted metabolomic analysis was performed with GC-MS and ^{1}H-NMR techniques. Further details are reported in the supplementary materials. The Krebs' cycle intermediates were analyzed with a targeted approach through the GC-MS/MS technique. Technical information and the transitions of metabolites monitored are reported in Table 2 S.

XF Real-Time ATP assay (Seahorse)

The ATP production rates were measured using XF Real-time ATP Assay Kit (Agilent Technologies, CA, USA) according to the manufacturer's instructions. Based on the oxygen consumption and the extracellular acidification rate, this assay measures real-time ATP production from the two major bioenergetics pathways, glycolysis and mitochondrial respiration. Additional technical information is reported in the supplementary materials.

Multivariate and univariate statistical analysis

Multivariate statistical data analysis was performed using SIMCA version 17.0 (U Sartorius Stedim Biotech, Umea, Sweden). First, data underwent a Principal Component Analysis (PCA), which is important for the investigation of sample distributions without classification. The univariate statistical analysis was performed using GraphPad Prism software (version 7.01, GraphPad Software, Inc., CA, USA). A Student's t-test or ANOVA test was performed to evaluate statistical significance and a p-value ≤ 0.05 was considered statistically significant. Data are presented as means ± standard deviation. All experiments were performed three times independently, each time at least in triplicate. Results were considered significant when * $p < 0.05$, ** $p < 0.01$, *** $p < 0.001$, **** $p < 0.0001$.

Data availability

The data produced and/or analyzed during the current study are available from the corresponding author on reasonable request.

Received: 6 June 2025; Accepted: 15 September 2025
Published online: 23 October 2025

References

1. Bray, F. et al. Global cancer statistics 2022: GLOBOCAN estimates of incidence and mortality worldwide for 36 cancers in 185 countries. *CA Cancer J. Clin.* **74**, 229–263 (2024).
2. Rawla, P., Sunkara, T. & Barsouk, A. Epidemiology of colorectal cancer: incidence, mortality, survival, and risk factors. *Prz Gastroenterol.* **14**, 89–103 (2019).
3. Siegel, R. L., Wagle, N. S., Cercek, A. & Smith, R. A. Jemal, A. Colorectal cancer statistics, 2023. *CA Cancer J. Clin.* **73**, 233–254 (2023).
4. Hanahan, D. & Weinberg, R. A. Hallmarks of cancer: the next generation. *Cell* **144**, 646–674 (2011).
5. Brown, R. E., Short, S. P. & Williams, C. S. Colorectal cancer and metabolism. *Curr. Colorectal Cancer Rep.* **14**, 226–241 (2018).
6. Wei, Z., Liu, X., Cheng, C., Yu, W. & Yi, P. Metabolism of amino acids in cancer. *Front. Cell. Dev. Biol.* **8**, 603837 (2021).
7. Still, E. R., Yuneva, M. O. & Correction Hopefully devoted to Q: targeting glutamine addiction in cancer. *Br J Cancer.* 120, 957 Erratum for: *Br J Cancer.* 2017 116, 1375–1381 (2017). (2019).
8. Spada, M. et al. Glutamine Starvation Affects Cell Cycle, Oxidative Homeostasis and Metabolism in Colorectal Cancer Cells. *Antioxidants*. 10, 683 (2023).
9. Katt, W. P., Lukey, M. J. & Cerione, R. A. A tale of two glutaminases: homologous enzymes with distinct roles in tumorigenesis. *Future Med Chem.* 9, 223–243 Erratum in: *Future Med Chem.* 9, 527 (2017). (2017).
10. Masisi, B. K. et al. The role of glutaminase in cancer. *Histopathology* **76**, 498–508 (2020).
11. Huang, F., Zhang, Q., Ma, H., Lv, Q. & Zhang, T. Expression of glutaminase is upregulated in colorectal cancer and of clinical significance. *Int. J. Clin. Exp. Pathol.* **15**, 1093–1100 (2014).
12. Xiang, L. et al. Glutaminase 1 expression in colorectal cancer cells is induced by hypoxia and required for tumor growth, invasion, and metastatic colonization. *Cell. Death Dis.* **10**, 40 (2019).
13. Choi, Y. K. & Park, K. G. Targeting glutamine metabolism for cancer treatment. *Biomol. Ther.* **26**, 19–28 (2018).
14. Chen, Y. et al. Targeting glutaminase 1 (GLS1) by small molecules for anticancer therapeutics. *Eur. J. Med. Chem.* **252**, 115–306 (2023).
15. https://clinicaltrials.gov/search?term=CB839&cond=Cancer&viewType=Table
16. Harding, J. J. et al. A phase I Dose-Escalation and expansion study of Telaglenastat in patients with advanced or metastatic solid tumors. *Clin. Cancer Res.* **27**, 4994–5003 (2021).
17. Lee, C. H. et al. Telaglenastat plus everolimus in advanced renal cell carcinoma: A Randomized, Double-Blinded, Placebo-Controlled, phase II ENTRATA trial. *Clin. Cancer Res.* **28**, 3248–3255 (2022).
18. Tannir, N. M. et al. Efficacy and safety of Telaglenastat plus Cabozantinib vs placebo plus Cabozantinib in patients with advanced renal cell carcinoma: the CANTATA randomized clinical trial. *JAMA Oncol.* **8**, 1411–1418 (2022).
19. Cohen, A. S. et al. Combined Blockade of EGFR and glutamine metabolism in preclinical models of colorectal cancer. *Transl Oncol.* **13**, 100–828 (2020).
20. Gaglio, D. et al. Disruption of redox homeostasis for combinatorial drug efficacy in *K-Ras* tumors as revealed by metabolic connectivity profiling. *Cancer Metab.* **8**, 22 (2020).
21. Hao, Y. et al. Oncogenic PIK3CA mutations reprogram glutamine metabolism in colorectal cancer. *Nat. Commun.* **7**, 11971 (2016).
22. Kandasamy, P. et al. Oncogenic KRAS mutations enhance amino acid uptake by colorectal cancer cells via the Hippo signaling effector YAP1. *Mol. Oncol.* **15**, 2782–2800 (2021).
23. Polat, I. H. et al. Glutamine modulates expression and function of glucose 6-Phosphate dehydrogenase via NRF2 in colon cancer cells. *Antioxidants* **10**, 1349 (2021).
24. Toda, K. et al. Metabolic alterations caused by KRAS mutations in colorectal cancer contribute to cell adaptation to glutamine depletion by upregulation of asparagine synthetase. *Neoplasia* **18**, 654–665 (2016).
25. Chao, H. X. et al. Orchestration of DNA damage checkpoint dynamics across the human cell cycle. *Cell. Syst.* **5**, 445–459 (2017).
26. Shen, Y. A. et al. Inhibition of the MYC-Regulated glutaminase metabolic axis is an effective synthetic lethal approach for treating chemoresistant ovarian cancers. *Cancer Res.* **80**, 4514–4526 (2020).
27. Diehl, F. F. et al. Nucleotide imbalance decouples cell growth from cell proliferation. *Nat. Cell Biol.* **24**, 1252–1264 (2022).
28. Fu, S. et al. Glutamine synthetase promotes radiation resistance via facilitating nucleotide metabolism and subsequent DNA damage repair. *Cell. Rep.* **28**, 1136–1143 (2019).
29. Hu, J. et al. Glutamine metabolism in the proliferation of GS-expression pituitary tumor cells. *Endocr. Connect.* **9**, 223–233 (2020).
30. Tardito, S. et al. Glutamine synthetase activity fuels nucleotide biosynthesis and supports growth of glutamine-restricted glioblastoma. *Nat. Cell. Biol.* **17**, 1556–1568 (2015).
31. Fuchs, B. C. & Bode, B. P. Stressing out over survival: glutamine as an apoptotic modulator. *J. Surg. Res.* **131**, 26–40 (2006).
32. Matés, J. M., Segura, J. A., Alonso, F. J. & Márquez, J. Pathways from glutamine to apoptosis. *Front. Biosci.* **11**, 3164–3180 (2006).
33. Chen, L. & Cui, H. Targeting glutamine induces apoptosis: A cancer therapy approach. *Int. J. Mol. Sci.* **16**, 22830–22855 (2015).
34. Jiang, B. et al. Filamentous GLS1 promotes ROS-induced apoptosis upon glutamine deprivation via insufficient asparagine synthesis. *Mol. Cell.* **82**, 1821–1835 (2022).
35. Kopeć, K. K. et al. Unlocking the secrets of metabolomics with artificial intelligence: a comprehensive literature review. *J. Pediatr. Neonat Individual Med.* **13**, 130105 (2024).
36. Macias, R. I. R. et al. A novel serum metabolomic profile for the differential diagnosis of distal cholangiocarcinoma and pancreatic ductal adenocarcinoma. *Cancers* **12**, 1433 (2020).

37. Ioannou, G. N., Nagana Gowda, G. A., Djukovic, D. & Raftery, D. Distinguishing NASH histological severity using a multiplatform metabolomics approach. *Metabolites* **10**, 168 (2020).
38. Piras, C. et al. Metabolomics analysis of plasma samples of patients with fibromyalgia and electromagnetic sensitivity using GC-MS technique. *Sci. Rep.* **12**, 21923 (2022).
39. Murgia, F. et al. Metabolomic changes in patients affected by multiple sclerosis and treated with Fingolimod. *Metabolites* **13**, 428 (2023).
40. Swietlik, E. M. et al. Plasma metabolomics exhibit response to therapy in chronic thromboembolic pulmonary hypertension. *Eur. Respir J.* **57**, 2003201 (2021).
41. Wishart, D. S. Metabolomics for investigating physiological and pathophysiological processes. *Physiol. Rev.* **99**, 1819–1875 (2019).
42. Gross, M. I. et al. Antitumor activity of the glutaminase inhibitor CB-839 in triple-negative breast cancer. *Mol. Cancer Ther.* **13**, 890–901 (2014).
43. Nong, S. et al. Mechanism and application of nonessential amino acid deprivation associated with tumor therapy. *MedComm - Future Med.* **1**, 2 (2022).
44. Soh, H., Wasa, M., Wang, H. S. & Fukuzawa, M. Glutamine regulates amino acid transport and glutathione levels in a human neuroblastoma cell line. *Pediatr. Surg. Int.* **21**, 29–33 (2005).
45. Zhou, Y., Jetton, T. L., Goshorn, S., Lynch, C. J. & She, P. Transamination is required for {alpha}-ketoisocaproate but not leucine to stimulate insulin secretion. *J. Biol. Chem.* **285**, 33718–33726 (2010).
46. Polet, F. et al. Reducing the Serine availability complements the Inhibition of the glutamine metabolism to block leukemia cell growth. *Oncotarget* **7**, 1765–1776 (2016).
47. Tanaka, K. et al. Glioma cells require one-carbon metabolism to survive glutamine starvation. *Acta Neuropathol. Commun.* **9**, 16 (2021).
48. Fadaka, A. et al. Biology of glucose metabolization in cancer cells. *J. Oncological Sci.* **3**, 45–51 (2017).
49. Timofeeva, N. et al. Preclinical investigations of the efficacy of the glutaminase inhibitor CB-839 alone and in combinations in chronic lymphocytic leukemia. *Front. Oncol.* **13**, 1161254 (2023).
50. Usart, M. et al. The glutaminase inhibitor CB-839 targets metabolic dependencies of JAK2-mutant hematopoiesis in MPN. *Blood Adv.* **8**, 2312–2325 (2024).
51. Kumar, A. et al. NaCT/SLC13A5 facilitates citrate import and metabolism under nutrient-limited conditions. *Cell. Rep.* **36**, 109701 (2021).
52. Hoang, G. et al. Uncovering metabolic reservoir cycles in MYC-transformed lymphoma B cells using stable isotope resolved metabolomics. *Anal. Biochem.* **632**, 114206 (2021).
53. Salminen, A., Jouhten, P., Sarajärvi, T., Haapasalo, A. & Hiltunen, M. Hypoxia and GABA shunt activation in the pathogenesis of alzheimer's disease. *Neurochem Int.* **92**, 13–24 (2016).
54. Bown, A. W. & Shelp, B. J. Does the GABA shunt regulate cytosolic GABA? *Trends Plant. Sci.* **25**, 422–424 (2020).
55. Kulkarni, C. A. & Brookes, P. S. Cellular compartmentation and the Redox/Nonredox functions of NAD. *Antioxid. Redox Signal.* **31**, 623–642 (2019).
56. Navas, L. E. & Carnero, A. Nicotinamide adenine dinucleotide (NAD) metabolism as a relevant target in cancer. *Cells* **11**, 2627 (2022).
57. Yaku, K., Okabe, K., Hikosaka, K. & Nakagawa, T. NAD metabolism in cancer therapeutics. *Front. Oncol.* **8**, 622 (2018).
58. Kim, D. H., Kim, D. J., Park, S. J., Jang, W. J. & Jeong, C. H. Inhibition of GLS1 and ASCT2 synergistically enhances the anticancer effects in pancreatic cancer cells. *J. Microbiol. Biotechnol.* **35**, 1–12 (2025).
59. Ren, L. et al. Glutaminase-1 (GLS1) Inhibition limits metastatic progression in osteosarcoma. *Cancer Metab.* **8**, 4 (2020).
60. Reis, L. M. D. et al. Dual Inhibition of glutaminase and carnitine palmitoyltransferase decreases growth and migration of glutaminase Inhibition-resistant triple-negative breast cancer cells. *J. Biol. Chem.* **294**, 9342–9357 (2019).
61. Serreli, G. et al. Ferulic acid metabolites attenuate LPS-Induced inflammatory response in Enterocyte-like cells. *Nutrients* **13**, 3152 (2021).
62. Dettori, T. et al. Synthesis and antiproliferative effect of halogenated coumarin derivatives. *Molecules* **27**, 8897 (2022).
63. Santoru, M. L. et al. Modulatory effect of nicotinic acid on the metabolism of Caco-2 cells exposed to IL-1β and LPS. *Metabolites* **10**, 204 (2020).
64. Tronci, L. et al. Vitamin C cytotoxicity and its effects in redox homeostasis and energetic metabolism in papillary thyroid carcinoma cell lines. *Antioxidants* **10**, 809 (2021).

Acknowledgements

We acknowledge the CeSAR (Centro Servizi Ricerca d'Ateneo) core facility of the University of Cagliari and Dr. Rita Pillai for assistance with the generation of the flow cytometry data.

Author contributions

M.S.: Conceptualization, Methodology, Formal analysis, Investigation, Data Curation Writing - Original Draft, Visualization, Project administration. C.P.: Methodology, Formal analysis, Writing - Review & Editing. V.P.L.: Conceptualization, Formal analysis, Investigation, Writing - Review & Editing, Visualization. M.C.: Methodology, Formal analysis, Writing - Original Draft. G.S.: Conceptualization, Methodology, Formal analysis, Writing - Review & Editing. A.N.: Writing - Review & Editing. K.L.: Methodology. K.K.K.: Formal analysis. G. Serreli: Writing - Review & Editing. F.M.: Writing - Review & Editing. F.E.: Methodology. T.D.: Writing - Review & Editing. L.A.: Conceptualization, Writing - Review & Editing, Supervision, Project administration. P.C.: Conceptualization, Writing - Review & Editing, Supervision, Project administration.

Funding sources

This research did not receive any specific grant from funding agencies in the public, commercial, or not-for-profit sectors.

Declarations

Competing interests

The authors declare no competing interests.

Additional information

Supplementary Information The online version contains supplementary material available at https://doi.org/1

0.1038/s41598-025-20528-2.

Correspondence and requests for materials should be addressed to C.P.